



Kent Academic Repository

Yoh, Natalie, Haley, Charlotte L. and Burivalova, Zuzana (2024) *Time series methods for the analysis of soundscapes and other cyclical ecological data.* *Methods in Ecology and Evolution*, 15 (7). pp. 1158-1176.

Downloaded from

<https://kar.kent.ac.uk/106239/> The University of Kent's Academic Repository KAR

The version of record is available from

<https://doi.org/10.1111/2041-210x.14361>

This document version

Publisher pdf

DOI for this version

Licence for this version

CC BY-NC (Attribution-NonCommercial)

Additional information

Versions of research works

Versions of Record

If this version is the version of record, it is the same as the published version available on the publisher's web site. Cite as the published version.

Author Accepted Manuscripts

If this document is identified as the Author Accepted Manuscript it is the version after peer review but before type setting, copy editing or publisher branding. Cite as Surname, Initial. (Year) 'Title of article'. To be published in ***Title of Journal***, Volume and issue numbers [peer-reviewed accepted version]. Available at: DOI or URL (Accessed: date).

Enquiries

If you have questions about this document contact ResearchSupport@kent.ac.uk. Please include the URL of the record in KAR. If you believe that your, or a third party's rights have been compromised through this document please see our [Take Down policy](https://www.kent.ac.uk/guides/kar-the-kent-academic-repository#policies) (available from <https://www.kent.ac.uk/guides/kar-the-kent-academic-repository#policies>).

Time series methods for the analysis of soundscapes and other cyclical ecological data

Natalie Yoh^{1,2,3}  | Charlotte L. Haley⁴ | Zuzana Burivalova^{2,3} 

¹Durrell Institute of Conservation and Ecology, University of Kent, Canterbury, UK

²The Nelson Institute for Environmental Studies, University of Wisconsin-Madison, Madison, Wisconsin, USA

³Department of Forest and Wildlife Ecology, University of Wisconsin-Madison, Madison, Wisconsin, USA

⁴Argonne National Laboratory, Division of Mathematics and Computer Science, Lemont, Illinois, USA

Correspondence

Charlotte L. Haley
Email: chaley@anl.gov

Zuzana Burivalova
Email: burivalova@wisc.edu

Funding information

Argonne National Laboratory, Grant/Award Number: DE-AC02-06CH11357; Precious Forests Foundation; Prince Albert II of Monaco Foundation

Handling Editor: Marie Auger-Méthé

Abstract

1. Biodiversity monitoring has entered an era of 'big data', exemplified by a near-continuous collection of sounds, images, chemical and other signals from organisms in diverse ecosystems. Such data streams have the potential to help identify new threats, assess the effectiveness of conservation interventions, as well as generate new ecological insights. However, appropriate analytical methods are often still missing, particularly with respect to characterizing cyclical temporal patterns.
2. Here, we present a framework for characterizing and analysing ecological responses that represent nonstationary, complex temporal patterns and demonstrate the value of using Fourier transforms to decorrelate continuous data points. In our example, we use a framework based on three approaches (spectral analysis, magnitude squared coherence, and principal component analysis) to characterize differences in tropical forest soundscapes within and across sites and seasons in Gabon.
3. By reconstructing the underlying, cyclic behaviour of the soundscape for each site, we show how one can identify circadian patterns in acoustic activity. Soundscapes in the dry season had a complex diel cycle, requiring multiple harmonics to represent daily variation, while in the wet season there was less variance attributable to the daily cyclic patterns.
4. Our framework can be applied to most continuous, or near-continuous ecological data collected at a fine temporal resolution, allowing ecologists to explore patterns of temporal autocorrelation at multiple levels for biologically meaningful trends. Such methods will become indispensable as biological big data are used to understand the impact of anthropogenic pressures on biodiversity and to inform efforts to mitigate them.

KEYWORDS

bioacoustics, coherence, ecoacoustics, multitaper principal component analysis, passive acoustic monitoring, phenology, power spectrum estimation, tropical forest

This is an open access article under the terms of the [Creative Commons Attribution-NonCommercial](https://creativecommons.org/licenses/by-nc/4.0/) License, which permits use, distribution and reproduction in any medium, provided the original work is properly cited and is not used for commercial purposes.

© 2024 UChicago Argonne, LLC, Operator of Argonne National Laboratory and The Author(s). *Methods in Ecology and Evolution* published by John Wiley & Sons Ltd on behalf of British Ecological Society.

1 | INTRODUCTION

Conservation projects should strive to be evidence-informed, however, this often requires being able to effectively monitor biodiversity over time and space (Burivalova, Allnutt, et al., 2019; Downey et al., 2022; Martin et al., 2023). Advancements in battery capacities and data storage now enable passive detection technologies (e.g. acoustic detectors, camera traps) to collect biodiversity data autonomously at regular intervals over long periods of time (Burivalova et al., 2021; Bush, Sollmann, et al., 2017). For example, detectors can be used to profile the acoustic environment of a given location, from which we can extract information on the presence and absence of particular species, or simply the magnitude of acoustic activity across all sources via acoustic indices (Alcocer et al., 2022). An increasing number of projects collect long-term, continuous or near-continuous soundscape data across large geographic areas (Alcocer et al., 2022; Gage & Axel, 2014). Most projects, however, do not yet use the temporal aspect of the data to its full capacity, largely due to a lack of awareness about and accessibility of suitable statistical methods (Metcalf et al., 2021; Scarpelli et al., 2021; Wauchope et al., 2021).

Activity and diversity patterns across time are much less understood than patterns of diversity across space (Hillebrand et al., 2018; Socolar et al., 2016). Temporal activity varies at multiple scales and is often cyclical—from circadian, circalunar, to circannual (Gottesman et al., 2021; White & Hastings, 2020). Whereas circadian rhythms have been widely studied at an organism level (e.g. Häfker & Tessmar-Raible, 2020; Ince, 2022; Martinez-Bakker & Helm, 2015), there has rarely been a need to account for it in biodiversity monitoring studies. Such studies have previously typically captured only one 'snapshot' of biodiversity per day, or even per year, and long-term datasets are typically highly subsampled (Dornelas et al., 2014; Magurran et al., 2010). Even when longer-term datasets are available, such as in remote sensing, temporal auto-correlation is frequently overlooked, even though it may be just as ecologically important as spatial autocorrelation (Lewińska et al., 2023). For example, fruit trees may be spatially patchy across a landscape, dictating a frugivorous species' presence. However, the availability of food resources from these trees will also be restricted in time, not only spatially. In particular, cyclical patterns are important in ecological processes, with daily, monthly and seasonal cycles underlying the life histories of many organisms. First understanding such cyclical patterns is key to understanding how anthropogenic pressures can disrupt these cycles.

Changes in these cyclical patterns, as well as multi-year or decadal trends in diversity can be due to climate cycles such as El Niño, trophic dependencies like predator-prey cycles, or economic cycles that impact poaching or deforestation. Underlying ecological processes are still unknown for many phenological patterns across ecological systems, including in tropical forests (Davis et al., 2022; Sakai & Kitajima, 2019). Without such baseline information, it is challenging to correctly quantify the effects of disturbance on

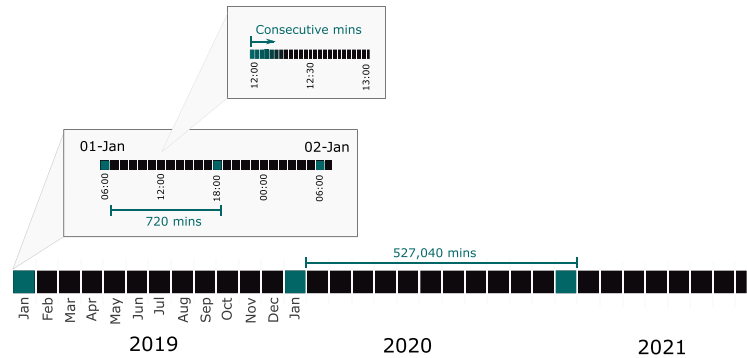
phenological patterns at the community or species level (Wauchope et al., 2021). Quantifying trends in variation (how much variation is normal), disentangling species' activity from species' presence, and understanding the processes contributing to these trends are fundamental questions in ecology, with profound consequences for conservation and the current extinction crisis (Gilbert et al., 2022; Magurran et al., 2010). For example, Carpenter and Brock (2006) suggested changes in the variance of seasonal phosphorus densities may act as an early ecological warning foreshadowing future eutrophication and a collapse in fish stocks.

Despite the importance of the temporal component, many studies average data points over large temporal bins, from 1 h, parts of the day, or entire days (Buxton et al., 2018; Fuller et al., 2015; Gage et al., 2017; Müller et al., 2023). While this may be suitable for certain questions, such as comparing the total daily activity across sites, it can also obscure important phenological patterns that may happen over short periods of time, such as several minutes. For example, the dawn chorus in acoustic activity in Indonesia is reflected by a sharp peak in the soundscape saturation index, but this peak becomes lower and broader following selective logging (Burivalova, Game, et al., 2019). Nor does binning time account for temporal autocorrelation, and binning can in fact be misleading because observations from contiguous time points are highly statistically dependent (Figure 1). As such, soundscape ecologists among others have called for future studies to standardize statistical approaches in soundscape analyses to consider responses across the diel cycle (Lawson et al., 2022).

There are many established statistical approaches for dealing with cyclical data, such as *spectral analysis* and *magnitude squared coherence* (Table 1). However, many of these approaches have not proliferated widely beyond specific sub-disciplines, such as palaeoecological modelling (Hammer, 2007), which commonly focus on back- or forecasting. Here, we demonstrate how a combination of spectral analysis, magnitude squared coherence, and principal component analysis can be used to characterize, analyse, and compare temporal, cyclical patterns present in ecological responses. As an example, we apply this framework to assess seasonal differences in the circadian patterns of soundscapes in Gabon's tropical forests. We (i) demonstrate why explicitly considering time in high temporal resolution data sets is necessary and advantageous; (ii) using spectral analysis in the time domain, we then characterize the daily cyclic behaviour of the soundscape for four sites in the dry season and four in the wet season in Gabon's forest; (iii) once we have characterized the cyclic behaviour and reconstructed it as a waveform, we use magnitude squared coherence to compare the magnitude of peaks in acoustic activity between two paired sites and (iv) assess the relative timing of these peaks between paired sites; and (v) finally, we compare the fundamental diel cycle observed across the dry season with that observed across the wet season using principal component analysis in the frequency domain. By exchanging time for frequency using a Fourier transform in this way, we are able to decorrelate otherwise contiguous observations. Combining these approaches enables us to quantify the

Three potential levels of temporal autocorrelation:

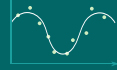
- Between consecutive minutes
- Repeating 12 hourly cycles (e.g. dawn & dusk)
- Repeating annual cycles (e.g. annual breeding seasons)



Framework for characterizing & comparing time series

Spectral analysis

- Use: Characterizes cyclical behaviour
- Extracts core temporal signal component
 - Removes noise or interference
 - Reconstructs the signal as a waveform



Magnitude-squared coherence

- Use: Computes correlation coefficients to compare two time series (two waveforms)
- Compares the relative timing or lead-lag behavior
 - Compares the relative amplitude of cycles/peaks



Principal component analysis

- Use: Quantifies the similarity between 3+ time series
- Reduces dimensionality to compare dominant signals
 - Identifies most important areas of variation between time series



Applications
We demonstrate this approach using soundscape data. Other forms of **quantitative continuous data** for which our approach is applicable:

FIGURE 1 Visualization of how temporal patterns may be interconnected and how our framework can be used to disentangle, characterize, and compare such patterns. A theoretical example could be differences in daily bird song rhythms across three sites. Bird song may exhibit a nested cyclical pattern where neighbouring minutes are temporally autocorrelated. However, there is also a cyclical pattern that repeats every 12h, which in turn is embedded within an annually repeating cycle. Therefore, we observe three tiers of temporal autocorrelation. (i) We can use spectral analysis to Fourier transform the data and characterize the core cyclical behaviour. Subsequently, we can (ii) use magnitude squared coherence to compare the relative timing and amplitude of bird activity between two sites, and (iii) use principal component analysis to identify the most important sources of variation in the cyclical patterns across all three sites.

cyclic behaviour of the soundscape, the variation observed within a site across several days, the variation observed across sites within a season, and the variation between seasons. We also apply these methods to a series of three simulated signals where the underlying cyclical behaviour is known for tutorial purposes. The accompanying code and data used for these analyses are available (see Data Availability Statement; Yoh et al. (2024a)).

2 | MATERIALS AND METHODS

2.1 | Demonstrating the need for temporal analysis

First, we demonstrate that potentially meaningful biological patterns may be diluted or lost if excessive binning of soundscape data is done in analyses. We do so by showing the same example

soundscape from two groups of sites at different levels of binning, for visual comparison.

2.2 | Temporal analysis summary

Next, using spectral analysis in the time domain, we characterize the daily cyclic behaviour of the soundscape for each site. Spectral analysis is used to identify oscillatory patterns within time series. It can be used to identify the core frequency components that make up these signals as spectra are generally understood to have two main features: one broad and smooth—the “continuum”, and the oscillations which cause large sharp peaks. In our example, the signal is the fluctuation of the acoustic index over time. *Frequency* in this context refers to the number of oscillations of a signal per unit of time, measured in cycles per day (cyc/d) (Table 1). For example, 1 cycle per

TABLE 1 Terminology reference table.

Terminology	Definition
Coherence	A complex quantity varying across frequency that measures the (linear) association between two jointly stationary time series
Discrete Fourier transform	A mathematical transformation to project a time-domain signal into a set of complex-valued coefficients of the Fourier series representation of the process at different frequencies. There are fast algorithms to compute the Fourier transform (fast Fourier transform, or FFT)
Frequency	The number of oscillations of a signal per unit of time (cyc/d). Not to be confused with acoustic frequency as a measure of sound (Hz)
Fundamental frequency (f_0)	The lowest frequency that can be given by a time series of length N , $1/N$
Harmonic of the frequency f_0	Positive integer multiples kf_0 where $k = 2, 3, \dots$
Magnitude squared coherence (MSC)	The squared magnitude of the coherence. Can be thought of as a frequency dependent correlation coefficient identifying oscillations at the same frequency common to both series. It ranges from 0 (no coherence) to 1 (perfect coherence, i.e. the two time series are related by a linear mechanism)
Periodogram	A statistical estimator for the power spectral density of a signal in the frequency domain. Periodograms may be computed with or without windowing (to reduce statistical bias), smoothing (to reduce variance of the estimator) and zero padding. The periodogram can be used to easily identify dominant frequencies in a signal
Phase	The relative timing or displacement between two signals at each frequency, measured in degrees. It is used to assess the lead/lag behaviour between two signals, and is especially of interest where the MSC is large
Power minus noise (PMN)	An acoustic index which quantifies the total energy of sound (dB) above background noise. For example the difference between the maximum decibel of each acoustic frequency bin and the corresponding decibel of the background noise profile for that bin
Power spectrum	Refers to the continuous-frequency representation of a stationary process that evolves through time in terms of its amplitude across frequency. Units are usually in units ² /Hz, where units here refer to the measurement unit of the original process
Principal component analysis (PCA)	A mathematical approach which aims to simplify complex data using data compression and dimension reduction. In this case, the PCA finds the cyclic behaviour common between multiple time series
Spectral analysis	A mathematical technique which decomposes the variance of a time series in terms of frequencies. The power spectrum contains the same information as the autocorrelation function, and in many applications can be simpler to interpret than the autocorrelations, especially when characterizing cyclic variation is of interest
Tapering	The process of pointwise multiplication of the time series x_t by a sequence of numbers v_n of the same length, before estimating the power spectrum or MSC
Waveform	In use in this paper to describe the result of estimating (by least squares) the amplitudes and phases of the sinusoidal components at 1 cyc/d, 2 cyc/d, ..., 12 cyc/d and adding them together to approximate the daily varying components of the time series
Zero-padding	The process of appending zeros to a time series before Fourier transforming. The spectrum or MSC that results from such a process has a smoother appearance because of special properties of the DFT but does not contain additional information

day would show a single peak and trough every 24h, two cycles per day would show a repeating 12-h pattern as this occurs twice per day (e.g. dusk and dawn calling behaviour), and so on. The sampling rate is one soundscape index value per minute for a total of 1440 data points.

To estimate the *power spectrum* (Table 1), the squared magnitude of the Fourier transform of the time series (or periodogram) is computed to visualize the amplitude (or strength) of each frequency component within the signal. The periodogram partitions the variance of the signal as a function of frequency. The large peaks, that is local maxima, concisely show the frequencies that contribute the most variance to the signal. It may be that the signal is best described by a single frequency (e.g. just a cosine having one period every 24h) or it may be best described using a

combination of frequencies (e.g. by a weighted sum of cosines with 24-hour and 12-hour periods). We can then use these dominant oscillations to reconstruct the underlying *waveform* free of noise in the signal (i.e. random fluctuations in the data). This process is explained in greater detail under the subsection, *A single waveform: periodic reconstruction using spectral analysis*, but is mathematically equivalent to fitting a set of cosine curves with the relevant 24-h, 12-h period and so on, to the time series using least squares. Note that different combinations of harmonics with different corresponding weights can produce a broad range of waveform shapes, having few or many peaks/local maxima. Reconstructing the underlying waveform of a soundscape index helps us to characterize the fundamental behaviour of the soundscape for each season, free from noise in the signal.

When comparing two time series, *magnitude squared coherence* enables us to compute a correlation coefficient for each frequency (e.g. amplitude and consistency) and determine the relative timing, or lead-lag behaviour between each time series at that frequency (i.e. *phase*; Table 1). For example, two sites may experience a dawn chorus, but at site A it occurs at 05:00 whereas at site B it occurs at 06:00. This process is explained in greater detail under the subsection, *Comparing two waveforms: magnitude squared coherence*. Magnitude squared coherence is useful for comparing two time series but to compare across three or more time series, we can use *principal component analysis* or singular value decomposition (PCA) in the frequency domain. These techniques reduce dimensionality in order to compare dominant frequencies common to all series and identify the most important patterns of modes of variation in the data. This process is explained in greater detail under the subsection *Comparing two waveforms: principal component analysis*. In doing so, we can quantify the similarity of sites within a given season, as well as between seasons. This information can be used to determine whether there is a signal characteristic of, for example a forest soundscape in each season, which can then be used as a baseline to assess ecological disturbance in the area.

2.3 | A single waveform: Periodic reconstruction using spectral analysis

For the analysis of periodic components of time series, it is helpful to consider the Fourier series of the time series as well as its power spectrum estimate (Shumway et al., 2000, ch. 4.). Denote by x_t the time series of interest, where $t = 1, \dots, N$ and assume N is odd, for simplicity of the following expressions. The discrete Fourier series of the time series is defined as

$$x_t = a_0 + \sum_{j=1}^{(N-1)/2} a_j \cos(2\pi t j / N) + b_j \sin(2\pi t j / N) \quad (1)$$

where the a_j and b_j are given as

$$a_j = \frac{2}{N} \sum_{t=0}^{N-1} x_t \cos(2\pi t j / N) \quad (2)$$

$$b_j = \frac{2}{N} \sum_{t=0}^{N-1} x_t \sin(2\pi t j / N). \quad (3)$$

Alternatively, (1) can be written as

$$x_t = c_0 + \sum_{j=1}^{(N-1)/2} c_j \cos(2\pi t j / N + \phi_j) \quad (4)$$

where

$$c_j = \sqrt{a_j^2 + b_j^2} \quad (5)$$

$$\phi_j = \tan^{-1} \left(\frac{-b_j}{a_j} \right). \quad (6)$$

One can obtain the coefficients c_j and the phase ϕ_j by way of the *Discrete Fourier Transform*, defined as

$$d(j/N) = \frac{1}{\sqrt{N}} \sum_{t=1}^N x_t \exp(-2\pi i t j / N) \quad (7)$$

where $i = \sqrt{-1}$ (and $e^{i\theta} = \cos\theta + i\sin\theta$), so that

$$c_j = \frac{4}{N} |d(j/N)|^2 \quad (8)$$

$$\phi_j = \tan^{-1} \left(\frac{-\Im d(j/N)}{\Re d(j/N)} \right). \quad (9)$$

The series $|d(j/N)|^2$ is referred to as the *periodogram* which estimates a quantity called the *power spectrum* of a time series, and j/N is the frequency. The general interpretation of the periodogram of a time series is that it partitions the variance of the series as a function of frequency, that is, the value c_j where j/N corresponds to 1 cycle per day (cyc/d) represents the coefficient of a least squares regression of the oscillation with that frequency on the time series. One can also summarize the R^2 value from that oscillation by computing the ratio $c_j / \sum_k c_k$. For example a large peak at 1 cyc/d could be interpreted in the following way: a sinusoid with frequency of 1 cyc/d can be used to explain a large proportion of the variance of the series. Additional peaks at integer multiples of 1 cyc/d, for example 2 cyc/d, 3 cyc/d, ..., 12 cyc/d are called *harmonics of the fundamental frequency* at 1 cyc/d and make a substantial contribution to the variance of the signal. A likely reason we might see harmonics of 1 cyc/d is the signal is periodic with a 24-h period, but it is not perfectly sinusoidal, so additional harmonic components are necessary to capture the daily variation in the data. To get an idea of the total contribution of the circadian cycle in our example dataset, we reconstruct the oscillatory waveform (Bloomfield, 2000, ch. 2) computing the coefficients of Equation (4) for all eight sites but setting all but the relevant coefficients to zero, that is

$$y_t = c_0 + \sum_{jN=1, \dots, 12} c_j \cos(2\pi t j / N + \phi_j). \quad (10)$$

and c_0 is the sample mean, $\bar{x} = \sum_{t=0}^{N-1} x_t$, of the time series. In fact, the coefficients c_j would result following a least squares regression of the associated sinusoid $\cos(2\pi t j / N + \phi_j)$ on the time series x_t , so it is possible to assign an R-squared value to each of the sinusoids as well as the reconstructed waveform y_t . We will refer to the result of Equation (10) as the waveform reconstruction of the circadian cycle and allows one to characterize the contribution of the circadian pattern in the soundscapes separately from the residual component.

The periodogram can be implemented in standard computing packages (e.g. base R, or *astsa*) (Stoffer & Poison, 2024) using methods called *tapering*, *zero-padding* and *smoothing* (Shumway et al., 2000) which improve the statistical properties of the estimator.

In this paper, we have used only zero padding of the tools listed above to construct the periodograms, while smoothing was used in Bush, Abernethy, et al. (2017). Zero padding refers to appending zeros to the time series in order to increase the number of frequency bins in the periodogram, which causes a smoother, interpolated appearance, and allows for easier identification of the frequency intercept for large peaks. Data were detrended by subtracting the mean from the series before analyses. In later sections of this paper, we will employ the multitaper method (Thomson, 1982) which uses a set of K tapers. From the periodogram, we reconstructed the waveform and plotted this reconstruction atop the raw values for the acoustic index for comparison.

2.4 | Comparing two waveforms: Magnitude squared coherence

It is useful to compare two soundscapes, especially as regards to differences in the amplitudes and phases of the estimated waveforms. Such information informs us of the differences in the intensity of sound (e.g. the relative intensity of the dawn chorus) as well as the relative timing of cyclic patterns (e.g. the timing of the dawn chorus). For this, the magnitude squared coherence (Koopmans, 1995a; Shumway et al., 2000) is a useful tool. The general idea is that one can compute a correlation coefficient at every frequency to assess whether there is an oscillation common to both time series at that frequency. To estimate this, we first estimate the periodogram using the squared magnitude of $d(j/N)$, Equation (7), then we used the tapered time series to compute the multitaper eigencoefficient (Fourier transformed data), $\tilde{x}(f)$, where $f = j/N$ is a Fourier frequency, $j = 0, \dots, N-1$,

$$\tilde{x}(f) = \sum_{n=0}^{N-1} x_n v_n e^{-i2\pi fn/N} \quad (11)$$

where the data taper v_n is a standard cosine window. Then, supposing one has time series $x_{1,n}$ and $x_{2,n}$, one can compute their smoothed cross spectrum as:

$$S_{1,2}(f_k) = \sum_{k=-L}^L w_k \tilde{x}_1(f_k) \tilde{x}_2^*(f_k) \quad (12)$$

where \tilde{x}_i denotes Equation (11) computed using the i -th time series and $*$ denotes complex conjugation, that is $(a+bi)^* = (a-bi)$ where a and b are real. The weights w_k define the data taper of length $2L+1$. We have used the default smoothing from the R `astsa` package version 2.0. which matches `spec.pgram` from base-R, a modified Daniell smoother with parameter δ , to compute the MSC. We provide supplementary code which can be used to reproduce our analysis and the figures in the text. All analysis we have employed in R version 4.3.2 (R Core Team, 2023). Finally, the MSC was computed by using the ratio

$$c^2(f) = \frac{|S_{1,2}(f)|^2}{\sqrt{S_{1,1}(f)S_{2,2}(f)}} \quad (13)$$

and the phase was computed as

$$\phi(f) = \angle S_{1,2}(f) \quad (14)$$

where the angle notation in the above is accomplished in practice using the arctangent function that takes two arguments, the first being the negative imaginary part of $S_{1,2}(f)$ and the second being the real part of $S_{1,2}(f)$.

The Equation (13) can be interpreted as a correlation coefficient between the two series $x_{1,t}$ and $x_{2,t}$ at the frequency f . When there is high squared coherence, c^2 approaches unity, and the two series have a common oscillation at that frequency which can be related by a linear equation (Koopmans, 1995a). The phase at that frequency relates the leading or lagging relationship of the common oscillation from the series $x_{1,2}$ to the series $x_{2,t}$. We report phase in degrees in this paper but the phase can be converted to the relevant time index, for example hours, days or years by simply dividing the phase lag by the frequency of oscillation and converting from degrees to cycles by dividing again by 360° Koopmans (1995b, p. 138). For example, in the right plot of Figure 7, the 1 cyc/d frequency has a phase of 17.7° , which means that the IPA10ST data at 1 cyc/d leads the IPA11ST data by $24\text{h} \cdot 17.7^\circ/360^\circ = 1.18\text{h}$. Similarly, the 3 cyc/d frequency has a -27.7° phase, which means that the IPA10ST data at 1 cyc/d lags the IPA11ST data by $8\text{h} \cdot 27.7^\circ/360^\circ = 0.616\text{h}$. Note that the interpretation of the phase is only useful when the MSC is large at that frequency. Consult the accompanying code for more examples.

2.5 | Comparing two waveforms: Principal component analysis

For the analysis of more than two sites, we demonstrate the multitaper principal component analysis (PCA) method of Mann and Park (Mann & Park, 1999; Thomson, 1982). In comparison with the windows we used for frequency domain analysis thus far, this analysis uses the multitaper method that uses a set of orthogonal tapers, the discrete prolate spheroidal sequences (dpss) (Slepian, 1978; Thomson, 1982) as data windows. We will employ the R `multitaper` package (Rahim & Burr, 2013) with many of the default settings. The main effect of this choice of data windows is to cause peaks in the spectrum estimate to have a characteristic “square” appearance. Denoting the k th discrete prolate spheroidal sequence as $v_n^{(k)}$ for $n = 0, \dots, N-1$ and $k = 0, \dots, K-1$ where $K \leq 2NW$. Here, W is the bandwidth parameter which controls the statistical properties of the estimator (Percival & Walden, 2020), that is a large bandwidth admits less variance but more bias, whereas a small bandwidth admits more variance and less bias. In practical terms, a large sinusoidal component in a time series which produces a peak in the power spectrum will show up as an approximately “square” feature with a width of $2W$ cyc/d.

In the PCA method, we denote by $x_{j,t}$ where $j = 0, \dots, J-1$, $n = 0, \dots, N-1$ the j th time series, where we have first scaled each time series by subtracting the sample mean and dividing by the sample standard deviation. Compute first the Fourier transformed, windowed data as

$$X^{(j,k)}(f) = \sum_{n=0}^{N-1} x_{j,n} v_n^{(k)} e^{-2\pi i f n} \quad (15)$$

and collect the $X^{(j,k)}(f)$'s into a $J \times K$ matrix $\mathbf{X}(f)$. The spectral matrix $\mathbf{X}(f)^T \mathbf{X}(f)$ contains all of the spectra and cross spectra at the frequency f . We decompose the complex-valued $\mathbf{X}(f)$ as

$$\mathbf{X}(f) = \mathbf{U}(f) \mathbf{D}(f) \mathbf{V}(f) \quad (16)$$

which is called the principal component analysis of the matrix $\mathbf{X}(f)$. The complex-valued matrices $\mathbf{U}(f)$ and $\mathbf{V}(f)$ are $J \times J$ and $K \times K$, respectively, and contain the left and right singular vectors of the matrix $\mathbf{X}(f)$. The matrix $\mathbf{D}(f)$ is a real-valued $J \times J$ diagonal matrix containing the principal components of the spectral matrix. The principal components are to be interpreted as one interprets multitaper spectrum estimates.

The PCA method (also known as singular value decomposition, empirical orthogonal functions, or proper orthogonal decomposition) can be carried out on large numbers of time series to determine oscillatory components common to all series. The modifying amplitude and phase information encoded in the left singular vectors in $\mathbf{U}(f)$ contains the "spatial" information and the information in the right singular vectors, $\mathbf{V}(f)$ contains information specific to each of the orthogonal tapers. For the purposes of this paper, we are mainly concerned with the first axis of the PCA at every frequency, which is contained in the first row and column of $\mathbf{D}(f)$.

2.6 | Simulation study

In the following toy example, we have created a simulation to exemplify our methods on a dataset with known characteristics. Figure 2 shows three signals generated according to

$$s_t = 1.9084755 \cos(2\pi t - 1.51980198) + 3.0896019 \cos(2\pi t - 0.14755329) + 0.7874783 \cos(2\pi t - 0.04753097) \quad (17)$$

$$x_t = s_t + 1.457621 \zeta_t^1 \quad (18)$$

$$y_t = s_t + 2 \zeta_t^1 \quad (19)$$

$$z_t = 1.5 s_t + 3 \zeta_t^1 \quad (20)$$

where ζ_t^j is a white Gaussian noise process uncorrelated with the other ζ_t^k 's and t is a discrete index going from 0 to 7 in increments of $1/(60 \cdot 24)$ similar to 1 week of data sampled once per minute for a total of $N = 10080$ samples. The signals x_t , y_t and z_t all share the common deterministic signal s_t but with different amplitudes and different noise variances.

The left panel of Figure 3 shows the three power spectrum estimates of the data in Figure 2. The right panel of Figure 3 represents the simulated signals' first, second and third principal components. It is clear that the waveform, which creates the three large peaks in

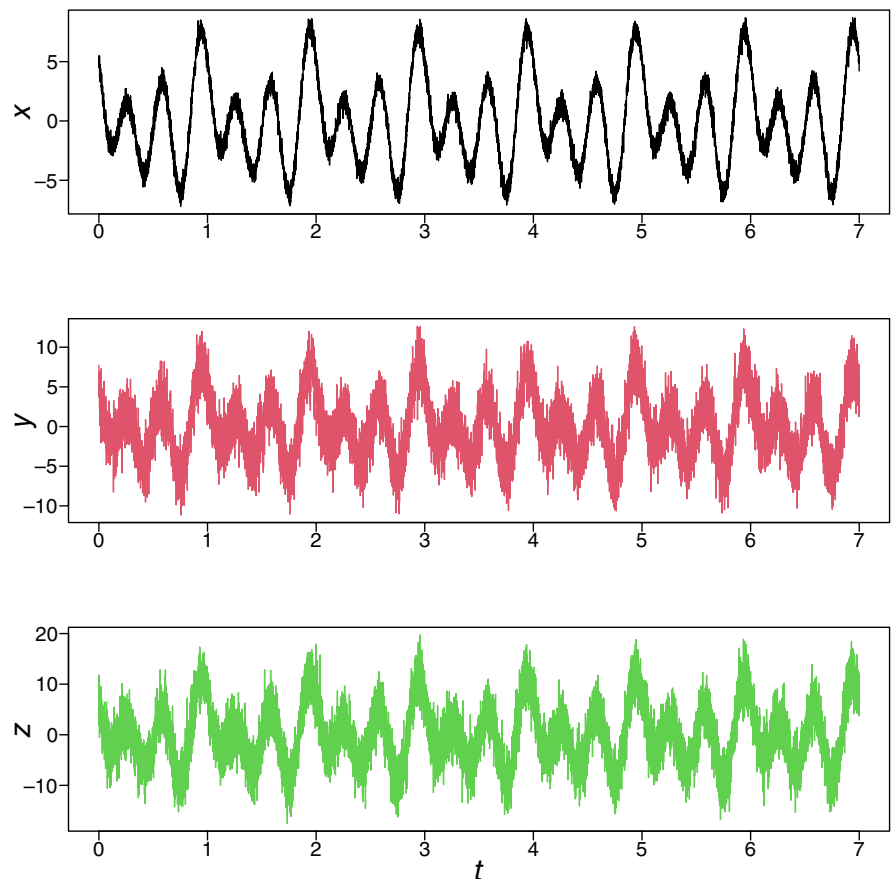


FIGURE 2 Three time series simulated according to Equation (17).

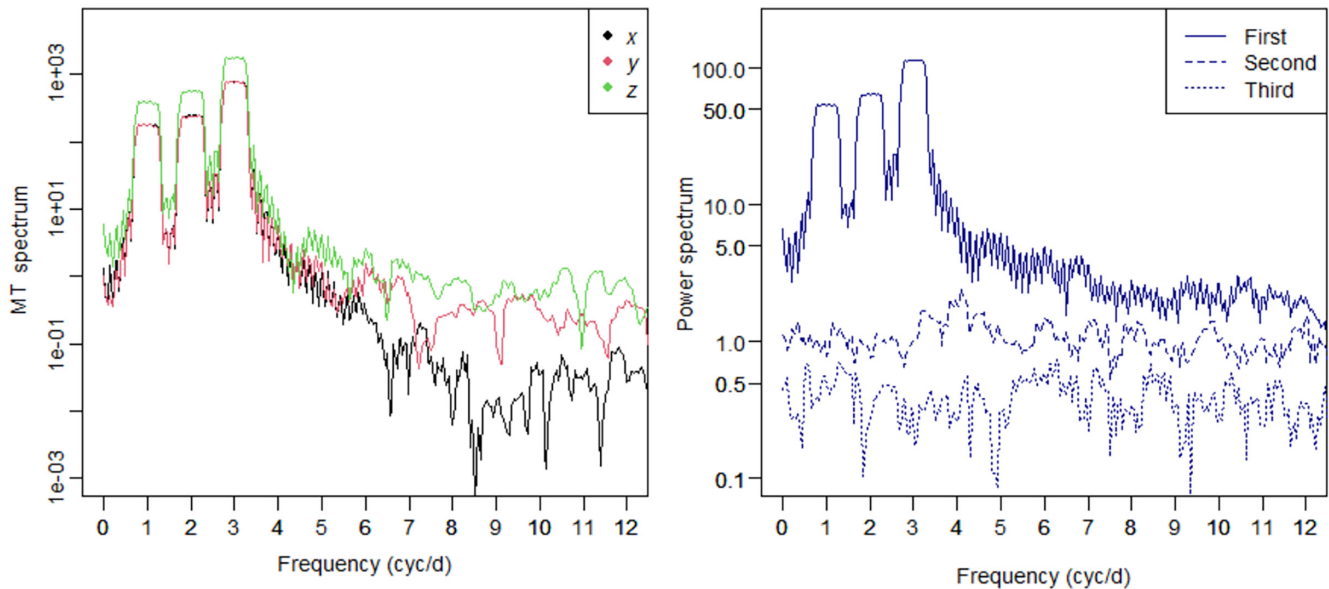


FIGURE 3 Left panel shows multitaper spectra of the three signals in [Figure 2](#). Right panel shows the MTM-PCA computed on the three time series, shown are the first three principal components in descending order of importance from solid, to dashed, to dotted. Note that all three oscillations are captured in the first principal component and the second and third reflect only noise.

the spectra left panel of [Figure 3](#), is entirely summarized by the first principal component.

2.7 | Main study data

We used acoustic data collected from eight sites in the Ogooué-Ivindo province of Gabon to demonstrate how time-series approaches can be leveraged to compare cyclical trends within and among groups of sites. All soundscape sampling occurred in closed, Gabonese rainforest with minimal habitat disturbance for at least 20 years prior to sampling. First, we sampled the soundscape in the wet season at four sites within Ivindo National Park, between February 19th and March 2nd 2021. Second, we sampled the soundscape in the dry season at four sites near Massaha between July 17, 2021 and July 23, 2021 (hereafter referred to as the Massaha sites, about 15 km from the Ivindo sites). At the time of sampling, the Massaha sites were located within a logging concession but no logging activity had commenced and there was an ongoing petition for the area to be re-designated as a community conservation area. At each site, we deployed one bioacoustic recorder to quantify the soundscape, separating each sampling site by at least 1 km to ensure independence. Sites were also positioned at least 200 m from roads, trails, and rivers. At each site, we deployed one bioacoustic recorder (BAR-LT, Frontier Labs) at 1.8 m above-ground, with a single omnidirectional microphone pointing down. Recorders were programmed for continuous, autonomous recording in 30-min segments for at least 6 days and set to record at 40 dB gain and a sample rate of 44.1 kHz. The day of deployment and collection were excluded from the analysis, to prevent the inclusion of human sounds and disturbance to the soundscape.

The data used here represents a subset from a larger project investigating the impacts of conservation areas, logging and hunting on soundscapes across Gabon (Yoh, Mbamy, et al., 2024). Here, we chose to present a subset of comparable sites to clearly outline our methodology and avoid introducing additional facets of complexity present across the whole dataset. Therefore, this study should only be viewed as a demonstration of the methodology. Please refer to Yoh, Mbamy, et al. (2024) which uses the full dataset to examine seasonal and land-use differences in forest soundscapes across Gabon. Fieldwork was carried out under permit AR017/20/MESRSTTENCFC/CENARET/CG/CST/CSAR, granted by Le Commissaire Général du Centre National de la Recherche Scientifique et Technologique (CENAREST).

To characterize the soundscape, we calculated the soundscape index *power minus noise* (PMN) for 256 acoustic frequency bins between 0 and 11 kHz (~43 Hz bandwidth each) and for each minute of the day, using 'AnalysisPrograms' (Towsey et al., 2020). PMN is the difference between the maximum decibel of each acoustic frequency bin and the corresponding decibel of the background noise profile (mean decibel level for that acoustic frequency bin; Towsey et al., 2014). Therefore, it provides a measure of the sound intensity for each acoustic frequency bin absent of background noise and provides a measure of acoustic activity. For further analyses, we summed all 256 PMN values for each minute of the day, yielding 1440 data points per day per site. We chose the PMN index as an example index in our time series analyses, because of its relatively simple interpretation and statistical properties. However, our approach could be applied to other acoustic indices commonly used in the literature, such as the acoustic complexity index (Alcocer et al., 2022; Bradfer-Lawrence et al., 2019).

3 | RESULTS

3.1 | Demonstrating the need for temporal analysis

Binning acoustic index data to coarser resolutions can significantly influence our interpretation of many temporal patterns (Figure 4). By binning the data to season we can infer that the dry season had a greater variance in PMN than the wet season, but there was no difference in mean PMN between seasons. By binning the data to day and night (05:00–17:00 and 17:00–05:00 respectively) we begin to see differences in daily variation in PMN between seasons (Figure 4). For instance, nightly PMN was higher in the dry season compared to PMN in the day but the same pattern is not observed for the wet season, where mean PMN was consistent between the two time periods. Further granularity, binning the data to hour, provides information about how this variation arises from across the day and night. We begin to see that the dry season exhibited a square waveform of medians with higher PMN throughout the night and the greatest variance during dawn and dusk. In contrast, PMN per hour was much more variable across the day in the wet season and the interquartile range was smaller at night. Breaking the data down to 15-min bins allows us to see the slope of change, particularly around dawn and dusk. Finally, plotting PMN continuously (per minute) allows us to see concentrated bands of activity for all periods of the day, as well as all outliers. However, it is very difficult to interpret visually as clusters of points obscure general patterns. Please note, boxplots should not be over-interpreted. Boxplots are usually produced with independent data, however here the data are from a time series and thus have high temporal correlation. Even though the effect of rain and different calling behaviours during the wet season are most likely explanations, the differences observed here could theoretically be caused by variables other than season, such as different forest structure between the sites, etc. However, our goal here is to demonstrate the approach on a simple set of sites, rather than infer the importance of different variables.

Binning over time can simplify data analysis and aid simple comparisons (e.g. overall PMN between seasons). However, it may sacrifice the ability to detect finer-grained variations and ecological relationships within the data. For example, aggregating PMN to day and night would mask the precise timing of the peak of the dawn chorus and the association between bird activity and sun irradiation. While the association of sun irradiation and avian vocal activity is well known (Gil & Llusia, 2020), other, as yet unknown patterns may be overlooked through excessive temporal binning.

3.2 | A single waveform: Periodic reconstruction of a waveform

Using PMN calculated on a per-minute basis, we characterized the daily cyclic behaviour of the soundscape for each site using spectral analysis (Figure 5). The reconstructed waveforms accounted for

25%–51% of the variance observed for signals in the dry season (R-squared values 0.513, 0.432, 0.342, and 0.253; Table S1) and approximately 15% in the wet season (R-squared values 0.155, 0.149, 0.041, and 0.156; Table S1), implying that the diel cycles comprise a much larger amount of the variance in the dry season than in the wet season. For one site in the wet season (IPA14ST), the waveform accounted only for 4% of the variance in PMN observed. The fact we can quantify the differences among seasons is a major result: in the wet season, other stochastic events in the soundscape account for a larger proportion of the variance in the signal than do the cyclic variations accounted for by the diel cycle. We do not observe meaningful differences in the sample mean or standard deviation between sites (Table S1). Considering the waveform fitted atop the raw values for PMN for one example site with the corresponding periodogram (Figure 5), it is apparent how the waveform is unaffected by the numerous outliers present in the data. The periodogram indicates that each frequency typically corresponds to a peak which means many harmonics are needed to reconstruct the mainly square waveform. The largest peak at 1 cyc/d indicates the main cyclic pattern repeats every 24 h in the dry season.

Considering all eight sites, the waveforms calculated using the Fourier series representation largely track the medians shown by the boxplots (Figure S1). Importantly, while the boxplots are a non-parametric estimate of the daily variation, the waveforms take into account the temporal correlations in the time series (Figure 4 while boxplots are agnostic to these correlations). Where the median of the boxplot and the waveform differ, we generally have outlying data points (e.g. midday IPA14ST). The waveforms help visualize differences in the cyclical behaviour of the soundscape between seasons (Figure S1). In the dry season, the waveform is square-shaped with high, consistent PMN at night, with two relatively small peaks at dawn and dusk. Diurnal PMN is substantially lower with minimal variation across the day. In contrast, the waveforms in the wet season typically have three peaks but both diurnal and nightly PMN oscillate along a mean value, which is consistent across the day. There is a peak in PMN during midday or afternoon, which is not present in the dry season.

3.3 | Comparing waveforms: Magnitude squared coherence

By plotting each of the eight waveforms together, we can visualize the similarity among sites more easily (Figure 6). There appears to be more coherence among sites in the dry season compared to the wet season, especially at dawn and dusk. Although we see the same three large peaks in PMN for each of the sites in the wet season, these peaks do not always occur concurrently or for the same length of time. We also see additional smaller peaks for certain sites that do not occur for others. If we compare waveforms between seasons, we observe that the dawn is associated with a downward slope during the dry season (i.e. acoustic activity decreases after sunrise) but an upward slope in the wet season (i.e. acoustic activity increases as the

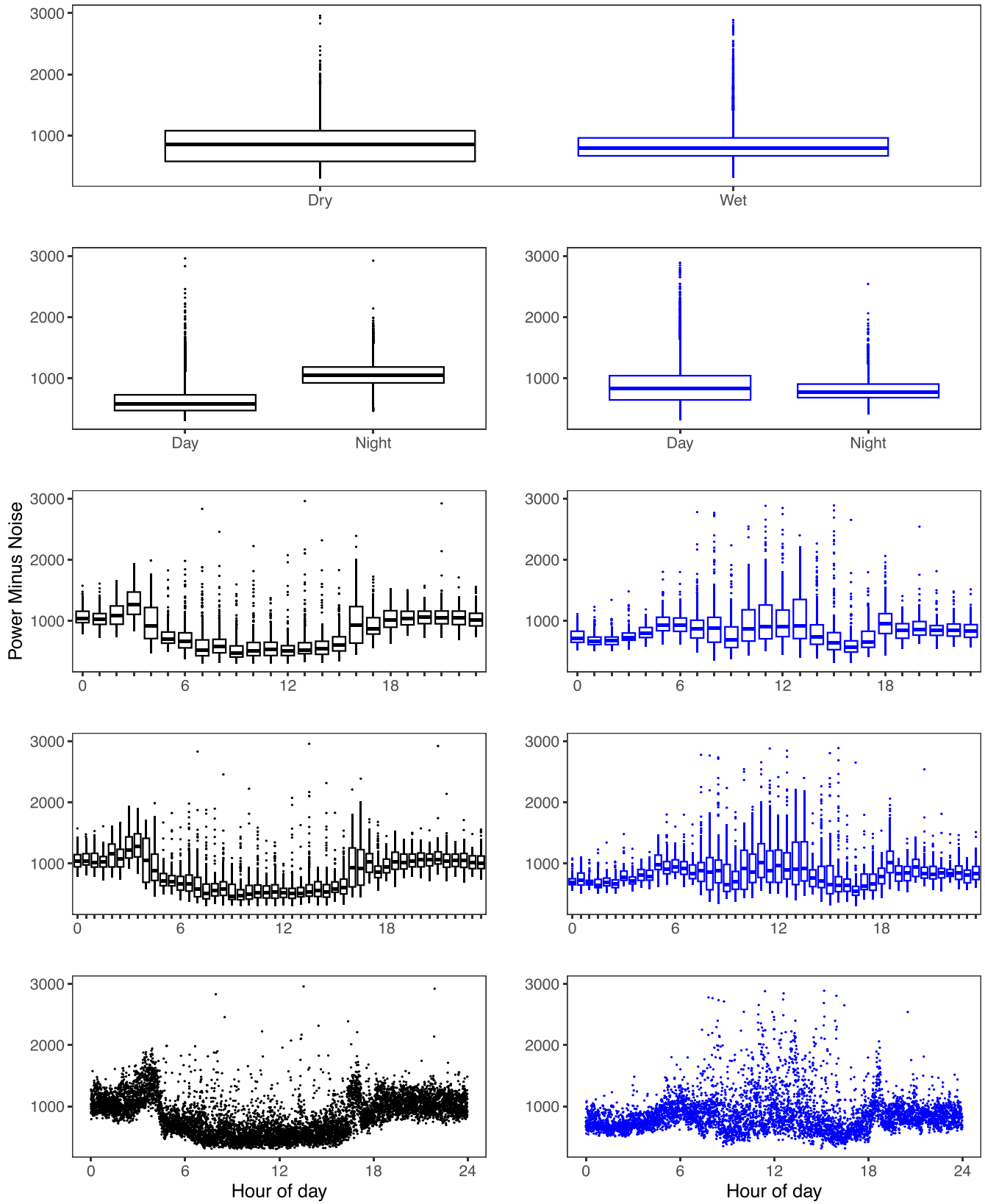


FIGURE 4 The acoustic index power minus noise (PMN) time series from eight sites, binned using various granularities, from the top: all data, day/night (05:00–17:00/17:00–05:00), hour, 15-min, and 1-min. Black boxplots correspond to time series from sites in the dry season, and black boxplots to those in the wet season.

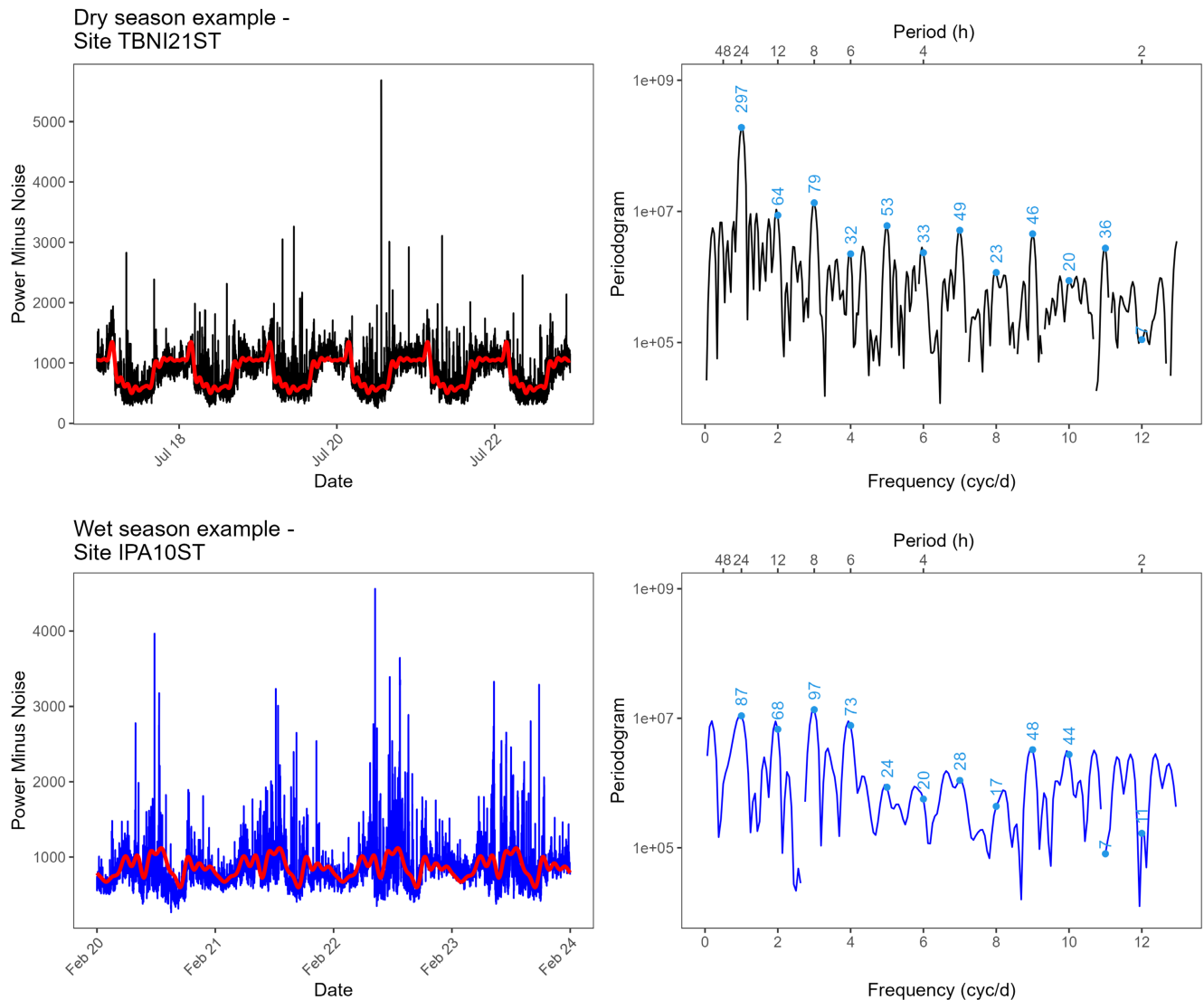


FIGURE 5 Right-hand panels show the power spectra generated for two example sites in the dry and wet season respectively, where the left-hand y-axis has logarithmic base-10 scaling. The left panels show the waveform atop the raw values of Power Minus Noise. The equation for the waveform is provided by Equation (10). The right panel shows the corresponding periodograms. The annotations above the periodograms give the amplitude of the periodogram at the 1, 2, ..., 12 cyc/d frequencies. Note the logarithmic base ten scale on the y-axis in the right panel, commonly used in the signal processing literature to make smaller features more visible and to show multiplicative effects as additive ones. Black and blue line colours represent time series from dry and wet seasons respectively.

sun rises). PMN increases during dusk as represented by an upward slope in both seasons.

To demonstrate how we can quantify common periodic components between sites, we computed magnitude squared coherence (MSC) comparing PMN, first between two sites within the same season (IPA10ST and IPA11ST) and second, between one site from each season (TBNI21ST and IPA10ST; Figure 7). The coherence between the two sites in the dry season was highly significant for at least six of the 12 harmonics. That is to say, the two time series are highly correlated at the harmonics of 1 cyc/d, 3 cyc/d, 4 cyc/d, 7 cyc/d, 8 cyc/d, and 12 cyc/d. Values of the MSC are to be interpreted like correlation coefficients; for example the value of 0.655 at 1 cyc/d exceeds the 99.99% point and represents an oscillation at 1 cyc/d common to both series. For

reference, were the true coherence zero (Shumway et al., 2000, Equation 4.105), the 99.99% significance level for the MSC would be 0.536, as shown by the top dotted horizontal line in Figure 7. All cyc/d reach the 90% significance level indicating high coherence across the day. The phase values (provided in the annotations in blue) also tended to be relatively flat near the harmonics of interest (e.g. 17.7° at 1 cyc/d), indicating a simple linear relationship at that frequency (e.g. peaks and troughs in PMN occur concurrently). As 1 cyc/d represents 24 h, a phase lag of 17.7° indicates that the peak in IPA11ST lags behind the peak in IPA10ST by approximately 1.18 h. Coherence is also high when comparing sites from both seasons (Figure 7 right). Whereas the two sites within the same season had a higher coherence overall, the two sites from different seasons still achieved coherence at the 90%

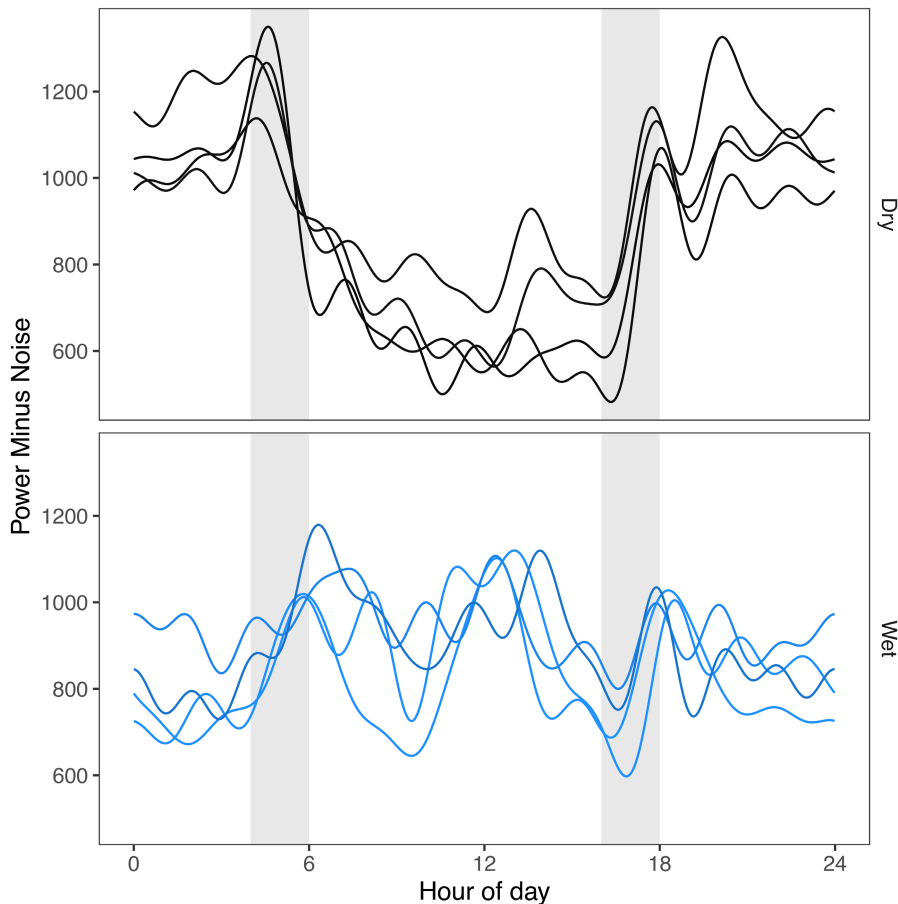


FIGURE 6 Each of the eight waveforms grouped by season to show dry (top panel) and wet (bottom panel) characteristics. The shaded grey bands represent dawn and dusk (04:00–6:00 and 16:00–18:00 respectively). One waveform represents one site.

level for nine of the 12 harmonics (excluding 9 cyc/d, 11 cyc/d, and 12 cyc/d). However, we observed greater differences in phase for at least five harmonics (3 cyc/d, 5 cyc/d, 6 cyc/d, 7 cyc/d, and 9 cyc/d), indicating differences in when peaks occur. For example, 6 cyc/d (corresponding to a 4-h cycle; see Figure 5) had a phase of -125.1° , indicating that this cycle occurred approximately 1.38 h earlier in TBNI21ST compared to IPA10ST.

3.4 | Comparing waveforms: Principal component analysis

We used PCA to compare the waveforms of more than two sites at a time. We computed the PCA for the four time series from the dry season and for the four time series from the wet season separately and compared the first and second principal components (Figure 8). The value of the first principal component encapsulated the dominant frequency domain information common to all sites in the wet and dry seasons respectively. For the wet season, there were peaks present for the first four cyc/d but no discernible pattern at higher harmonics. Principal components were marginally higher for 3 cyc/d and 4 cyc/d compared to 1 cyc/d and 2 cyc/d. In contrast, the PCA for the dry season showed peaks at 1 cyc/d, 3 cyc/d, 5 cyc/d, 7 cyc/d, 9 cyc/d and 11 cyc/d, though the peak at 1 cyc/d was much greater than at other harmonics. When we overlaid the first principal

component for both seasons, we saw that the peak at 1 cyc/d (24 h) was greater by a factor of three in the dry season compared to the wet season, whereas the principal component at 3 cyc/d (8 h) were very similar. The peak at 2 cyc/d (12 h) was missing from the dry season as the pseudo peak was less than $2W$ wide. So too the peak at 4 cyc/d (6 h) present in the wet season was absent from the dry season. As a whole, we observed that the dry season had a larger number of higher harmonics required to capture the variance reflective of the square nature of the waveforms.

4 | DISCUSSION

4.1 | Need for time series analysis

Here, we demonstrated a time series approach to characterize and quantify differences between cyclical, continuous data to explore meaningful ecological patterns. Using an example from Gabon's rainforest soundscapes during the dry and wet season, we demonstrated the need to carefully consider the temporal aspect of acoustic index data in ecological and conservation analyses. By aggregating the data, we lose information regarding cyclical patterns. In our example, if we only compare the acoustic index PMN using data binned to season, we may interpret the larger variation observed in the dry season to mean that sites in the dry season show

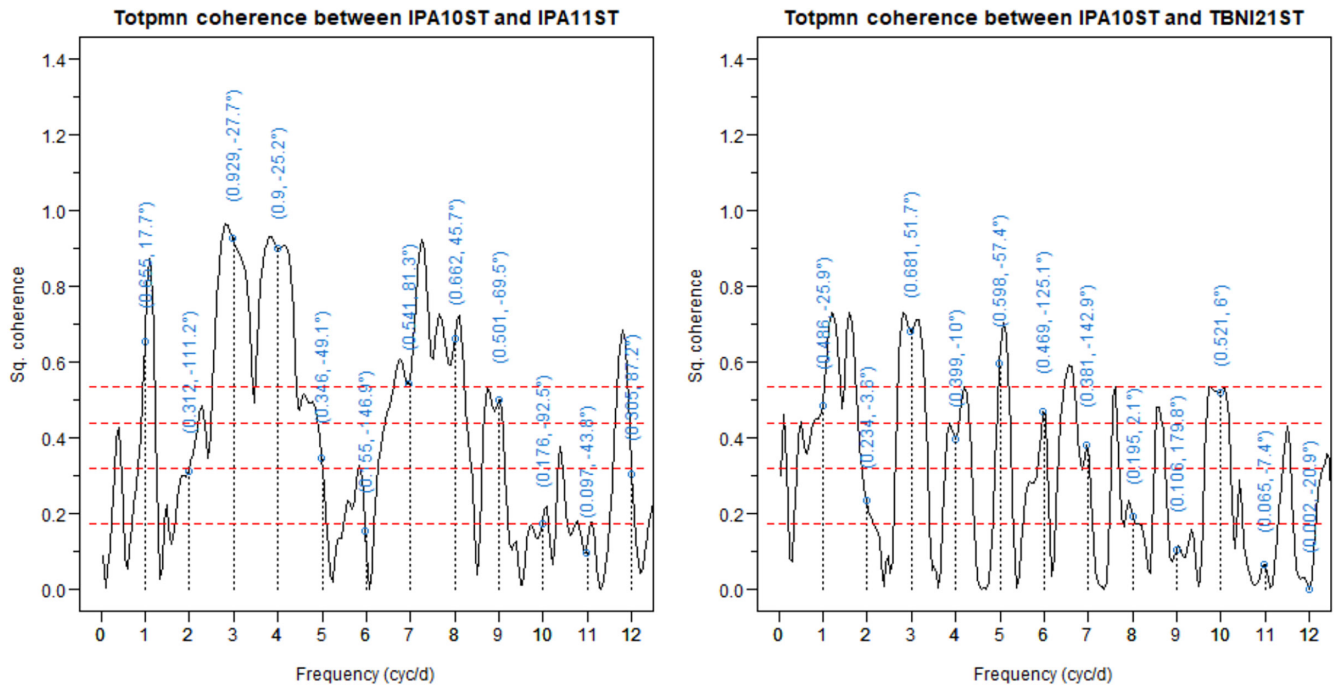


FIGURE 7 Magnitude squared coherence (MSC) between paired sites. The left plot shows the MSC and phase for two sites from the wet season (average squared coherence 0.465, IPA10ST and IPA11ST), and the right plot shows the MSC and phase for one site from each season (average squared coherence 0.345, IPA10ST and TBN121ST). Both plots have dotted horizontal lines indicating significance levels for the coherence, 90%, 99%, 99.9%, 99.99% (from bottom) assigned if the true coherence were zero. Dotted vertical lines indicate the 1 cyc/d fundamental and its harmonics, with blue annotations which give the coefficient c_k and phase angle (in degrees).

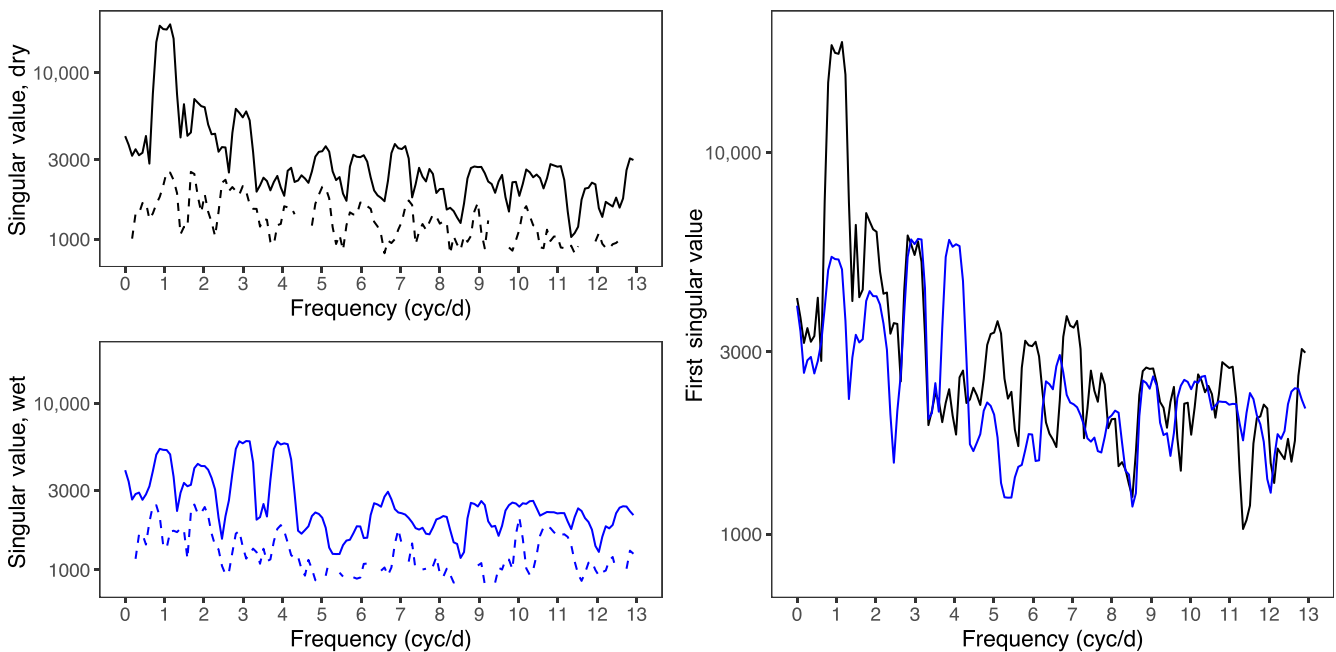


FIGURE 8 The multitaper principal component analysis (PCA) method, as in Equation (16), computed on two seasons. The first two principal components (first solid, second dashed) for four sites in the dry season (top left panel; black) and four sites in the wet season (bottom left panel; blue). The right panel shows the first principal components on the same plot.

greater dissimilarity compared to the wet season (Figure 4). When in fact, using the time series approach, we see that soundscapes in the dry season follow a more consistent daily pattern than those observed in the wet season. It is also possible to miss important trends

when binning data at a relatively fine temporal scale, such as 1 h. This in turn can prevent the understanding of the likely processes driving a temporal pattern in the data, for example in our case, a likely driver of the dawn chorus is sunrise (Gil & Llusia, 2020).

4.2 | Benefits over alternative methods

One of the greatest challenges of analysing time series is the interconnection between different periods of interest, in other words, different levels of temporal autocorrelation (Figure 1). Time series which relate to the earth's climate for example may fluctuate depending on daily and yearly cycles, but also solar cycles, tides, seismic effects and other periodic effects relating to geophysical phenomena. Biodiversity is inherently dependent on environmental stimuli so geophysical cycles will likely be embedded in cyclical, ecological patterns (Häfker & Tessmar-Raible, 2020; White & Hastings, 2020). In contrast, much of the statistical literature in other disciplines assumes that the time series is stationary, which, loosely speaking, means that the mean and variance of the time series does not change with time. This assumption is likely to be untrue when time series are observed over long periods and for many ecological questions. The ability to account for non-stationarity is more important than ever in ecological research as accelerating climate change continues to disrupt the exogenous cues dictating phenological behaviours (Davis et al., 2022; Morissette et al., 2009; Wuethrich, 2000).

In ecology, generalized additive models (GAMs) have gained popularity, due largely to their flexibility and relatively easy interpretation (Hastie & Tibshirani, 1990). Perhaps the largest uptake of GAMs has been in species distribution modelling, but they have also been used in network ecology, fisheries modelling, climate modelling and so forth. (Gleich et al., 2022; Guisan et al., 2002; Ravindra et al., 2019; Salazar et al., 2021). Accounting for temporal autocorrelation is possible within GAMs, that is by specifying an autoregressive model for errors, and it is possible to model cyclic patterns, such as by using cyclic cubic spline basis (Pedersen et al., 2019). However, choosing the appropriate model structure or level of smoothness can be challenging, and there are currently few examples of GAMs being applied to cyclical time series data in ecology (Salazar et al., 2021). Our method allows us to model this directly by using sines and cosines as basis functions, which has the distinct advantage that they can represent nonlinear dynamics using these functions as products of cosines that can be rewritten (using trigonometric identities) as linear combinations of cosine functions.

State-space models (SSM) remain one of the more readily adopted time series approaches used in ecology and they can provide a comprehensive way to estimate hidden processes in the data which may evolve over time (Bell et al., 2015). However, their computational and mathematical complexity presents a barrier to use for many ecologists (Auger-Méthé et al., 2021). Spectral analysis, implemented here, and state-space models are complementary time series approaches (Shumway et al., 2000). Spectral analysis focuses on identifying frequency components in a signal, while SSMs specify latent processes underlying the data. One assumption inherent in SSMs is that the observations are independent given the values of a latent, Markov process. Consequently, the primary objective of SSMs is to model the state itself. In combination, they can be used to gain a deeper understanding of the characteristics of time series data.

Dynamic time warping (DTW) is a technique that seeks to minimize the distance between two time series by expanding or contracting the temporal axis to find the closest fit between the two time series (Hegg & Kennedy, 2021). More generally, it can be used to cluster multiple time series into similar groups. Given adequate training data, DTW could potentially be used to classify a set of time series of soundscape data into a predefined number of categories. Similarly, tools such as Feature Analysis for Time Series (FATS; Nun et al., 2015) extract a set of predefined features from a time series that can be used to cluster or classify time series into groups. However, while DTW and FATS provide methods for classifying time series, they do not explicitly offer any insight into the periodic temporal correlations of the ecological processes involved, unlike PCA.

Similarly to our study, Bush, Abernethy, et al. (2017) demonstrate how to compute periodograms (with or without smoothing) on single time series, and show how to determine the significance of any given peak in the periodogram using a χ^2_2 distribution. Our work goes beyond this approach in the following ways: (i) We use the multitaper method for estimation of the frequency domain quantities of interest (spectrum, magnitude squared coherence, frequency domain principal component analysis), which is shown to be statistically more appropriate than smoothed periodograms (see Bronez, 1992; Percival & Walden, 2020; Thomson, 1982, and others from our bibliography). (ii) We show how to compute and interpret the magnitude squared coherence, which is a frequency-dependent quantity that allows one to compare two time series in terms of their common oscillatory components. (iii) The principal component analysis, computed in the frequency domain as in Mann & Park, 1999, is a powerful tool for combining information from many time series and is an excellent tool when moderately large numbers of time series are available. (iv) We compute the dominant waveforms of the diel cycles and can distinguish between the different site types by the waveform morphology. (v) Finally, we have packaged our code so that it is freely available for others to read and learn from and ultimately adapt to their own purposes.

4.3 | Potential uses in ecoacoustics and beyond

We used a simplified example from a limited number of sites and conditions (dry and wet season) to explain the methods, however, there are many opportunities where the method demonstrated here can be applied in ecology and conservation, using soundscape data and beyond. Fitting reconstructed waveforms and calculating the percentage of variance in the data that such a waveform captures can be particularly useful in monitoring, as it allows for easy identification of outliers and anomalies. For example, long-term acoustic recording programs, such as the Australian Acoustic Observatory (Roe et al., 2021), could monitor for changes in the r-squared values of individual site's waveforms, to alert researchers to meaningful changes in the soundscape composition. Such changes could be due to shifts in community composition, the arrival of invasive species, or new human disturbance (Gilbert et al., 2022). This approach

could complement deep learning methods for identifying anomalies in soundscapes (Sethi et al., 2020).

Being able to parameterize a model of an intact habitat's soundscape in terms of its daily phenology is important for conservation monitoring efforts that require measuring their effectiveness as compared to a control, or baseline (Burivalova, Game, et al., 2019). For example, reforestation projects may regularly compare the soundscapes of restored sites to soundscapes from intact forests, to gauge whether faunal communities are successfully returning along with regrowing trees (Vega-Hidalgo et al., 2021). Such comparisons (of a baseline and intervention condition) can be made using magnitude squared coherence, as demonstrated here. Many impact evaluation studies that use time series data rely on Before and After Control-Impact (BACI) models to compare change across paired time series. Methods exist to quantify changes in the mean, or in the linear trend and its change after intervention (Wauchope et al., 2021). However, these methods used typically in econometric analyses (Butsic et al., 2017), such as Difference in Difference, or fixed effects panel regressions, do not account for cyclical behaviour. Using magnitude squared coherence and principal component analysis builds on this approach and allows us to quantitatively compare non-linear responses, such as changes in daily phenology. For instance, whereas human disturbance of tropical forest in Indonesia was found to not change the daily mean of a soundscape index, it reduced the magnitude of the dawn and dusk peak, which was compensated with an increase in night-time index values (Burivalova et al., 2022).

As we demonstrate on the periodograms, it is also possible to estimate potential lags in biologically meaningful soundscape features (Figure 5). This could be useful, among others, for studies investigating the nocturnalization of species as a result of urbanization, acoustic niche partitioning among co-occurring bird species, or understanding and predicting the consequences of climate change for ecological communities (Gaynor et al., 2018; Inouye, 2022; Morissette et al., 2009; Planque & Slabbekoorn, 2008). Quantifying shifts in phenology is essential to environmental management. For example, the onset of spring has been trending earlier across many of the United States National Parks which in turn necessitates different approaches to management to help conserve the species they support (Monahan et al., 2016).

Our approach can help understand the underlying cyclical patterns in non-acoustic data with a lot of natural variation (Dröge et al., 2021). Flux towers measure the exchange of gases between ecosystems and the atmosphere (e.g. carbon dioxide, water vapour). These towers collect data at a high temporal resolution, capturing circadian and seasonal variations in ecosystem processes. Frequently, the temporal variation in data from flux towers is analysed using wavelet analysis (Schaller et al., 2017; Stoy et al., 2013). Wavelet methods allow the user to account for transient, local variations in the time series, and are appropriate for time series containing sharp discontinuities. While this approach is valuable, it may be challenging to implement and interpret by non-specialists, and it can be potentially sensitive to the choice of parameters, such as the type of wavelet, the number of decomposition levels,

and the scaling function. Similarly, sap flux data, providing insights into a tree's water transport dynamic, are cyclical with a circadian and seasonal pattern. While state-space models have been used to analyse sap flux data (Bell et al., 2015), our approach may help researchers compare for example the similarity among trees under different treatments. Other examples of high temporal resolution, cyclical data that our method may be useful for include outputs from animal behaviour data loggers (Soleymani et al., 2017; Williams et al., 2020), bird migration patterns from accelerometers (Barras et al., 2021; Pokrovsky et al., 2021), or satellite image measures such as Normalized Difference Vegetation Index (Recuero et al., 2019).

4.4 | Considerations in other contexts

Two considerations before using this approach include the continuity of the data and the distribution of the response variable. In this paper, we have demonstrated the methods using continuous data. However, we acknowledge that ecological data are often imperfect and there may be gaps due to survey equipment failure. While it is possible to deal with a limited number of gaps using the missing-data multitaper power spectrum estimator, as the number of gaps increases the model power decreases. It is beyond the scope of this paper to detail how to handle missing data, but we suggest that reliable results can be obtained when 30% or less of the data are missing, and there are four or fewer gaps, refer to Chave (2019, p. 2178) and Haley (2021, Example 1) for more information. Similarly, these methods assume the data are weakly stationary, where the mean value and variance stay constant over time.

4.5 | Future directions

Here we only characterized daily cyclical patterns, but future research should focus on nesting multiple layers of cyclicity in analyses, such as lunar and annual cycles or multiyear patterns (Figure 1). Such complexity becomes increasingly difficult to decipher using time bins, especially where the local mean and variance for a subset of the data may differ from the global mean and variance across a time series. By treating time as continuous, we are better able to identify and account for non-stationarity in the data whether that represents ecologically relevant cycles, such as seasonality, or natural variation, such as drift. This is particularly important for forecasting changes into the future.

In this paper, we demonstrate a nonparametric, frequentist exploratory analysis that could be a precursor to a Gaussian process framework. Gaussian processes (Rasmussen & Williams, 2006; Stein, 2005) offer an intriguing method for analysing spatiotemporal data. The main feature of the Gaussian process is that each observation is modelled as a realization of a Gaussian-distributed random variable, and then only the mean vector and covariance matrix need to be determined through the optimization of a set of parameters. While the Gaussian process approach has the potential to be widely

successful for such goals, for example prediction and smoothing, the specification of important quantities, such as the mean function and selecting the covariance function, are glossed over. In summary, the Gaussian Process method is a promising future direction for the modelling step of soundscape data, as it offers the possibility of encoding truly complex, nonstationary covariance structure with few parameters.

5 | CONCLUSIONS

Our spectral analysis approach provides a novel method for ecologists to explore the relationship between cyclical climatic and environmental conditions and their impacts on biological cyclical patterns. Many species' phenology, especially in tropical forests, remains poorly understood. Our method provides a tool to characterize geophysical and biological patterns, quantifying if and how they may be changing, and at what temporal scale. In doing so, this method can be used to detect the impact of disturbances and measure the effectiveness of a conservation intervention, at multiple ecologically meaningful timescales. Ultimately improving our understanding of phenological processes, we can better monitor changes in ecological conditions and thus inform conservation.

AUTHOR CONTRIBUTIONS

Zuzana Burivalova and Charlotte L. Haley conceived the ideas and designed the methodology; Zuzana Burivalova collected the data; Natalie Yoh processed the data; Charlotte L. Haley wrote the accompanying code and analysed the data; Natalie Yoh led the writing of the manuscript. All authors contributed critically to the drafts and gave final approval for publication.

ACKNOWLEDGEMENTS

The authors thank Walter Mbamy, Tatiana Satchivi, Médard Obiang Ebanega, Serge Ekazama Koto and Alex Ebang Mbélé for their fieldwork contributions. The authors also thank Sathya Chandra HS Sagara and Quinn Asena for their input and the reviewers for their valued comments. This project was funded by Precious Forests Foundation and Prince Albert II of Monaco Foundation to Z.B. This material is based upon work supported by the US Department of Energy, Office of Science, under contract number DE-AC02-06CH11357. The submitted manuscript has been created by UChicago Argonne, LLC, Operator of Argonne National Laboratory ("Argonne"). Argonne, a US Department of Energy Office of Science laboratory, is operated under Contract No. DE-AC02-06CH11357. The US Government retains for itself, and others acting on its behalf, a paid-up nonexclusive, irrevocable worldwide licence in said article to reproduce, prepare derivative works, distribute copies to the public, and perform publicly and display publicly, by or on behalf of the Government. The Department of Energy will provide public access to these results of federally sponsored research in accordance with the DOE Public Access Plan (<http://energy.gov/downloads/doe-public-access-plan>).

CONFLICT OF INTEREST STATEMENT

The authors have no conflict of interest.

PEER REVIEW

The peer review history for this article is available at <https://www.webofscience.com/api/gateway/wos/peer-review/10.1111/2041-210X.14361>.

DATA AVAILABILITY STATEMENT

Data available via the Dryad Digital Repository <https://doi.org/10.5061/dryad.xpnrx0kn6> (Yoh et al., 2024a). Code available via Zenodo <https://doi.org/10.5281/zenodo.11198178> (Yoh et al., 2024b).

STATEMENT ON INCLUSION

Our study was a methodological outline and therefore is not focused on addressing ecological questions for a specific region. However, we used data connected to a larger research project to demonstrate the approach. The larger project brings together authors from a number of different countries, including scientists based in the country where the study was carried out. However, we were unable to identify researchers in the region with the relevant statistical skills for this aspect of the project.

ORCID

Natalie Yoh  <https://orcid.org/0000-0002-6171-3800>

Zuzana Burivalova  <https://orcid.org/0000-0001-5730-7546>

REFERENCES

- Alcocer, I., Lima, H., Sugai, L. S. M., & Llusia, D. (2022). Acoustic indices as proxies for biodiversity: A meta-analysis. *Biological Reviews*, 97(6), 2209–2236.
- Auger-Méthé, M., Newman, K., Cole, D., Empacher, F., Gryba, R., King, A. A., Leos-Barajas, V., Mills Flemming, J., Nielsen, A., Petris, G., & Thomas, L. (2021). A guide to state-space modeling of ecological time series. *Ecological Monographs*, 91(4), e01470.
- Barras, A. G., Liechti, F., & Arlettaz, R. (2021). Seasonal and daily movement patterns of an alpine passerine suggest high flexibility in relation to environmental conditions. *Journal of Avian Biology*, 52(12), 321–335.
- Bell, D. M., Ward, E. J., Oishi, A. C., Oren, R., Flikkema, P. G., & Clark, J. S. (2015). A state-space modeling approach to estimating canopy conductance and associated uncertainties from sap flux density data. *Tree Physiology*, 35(7), 792–802.
- Bloomfield, P. (2000). *Fourier analysis of time series: An introduction*. John Wiley & Sons.
- Bradfer-Lawrence, T., Gardner, N., Bunnefeld, L., Bunnefeld, N., Willis, S. G., & Dent, D. H. (2019). Guidelines for the use of acoustic indices in environmental research. *Methods in Ecology and Evolution*, 10(10), 1796–1807.
- Bronez, T. P. (1992). On the performance advantage of multitaper spectral analysis. *IEEE Transactions on Signal Processing*, 40(12), 2941–2946.
- Burivalova, Z., Allnutt, T. F., Rademacher, D., Schlemm, A., Wilcove, D. S., & Butler, R. A. (2019). What works in tropical forest conservation, and what does not: Effectiveness of four strategies in terms of environmental, social, and economic outcomes. *Conservation Science and Practice*, 1(6), e28.
- Burivalova, Z., Game, E. T., & Butler, R. A. (2019). The sound of a tropical forest. *Science*, 363(6422), 28–29.

- Burivalova, Z., Maeda, T., Rayadin, Y., Boucher, T., Choksi, P., Roe, P., Truskinger, A., & Game, E. (2022). Loss of temporal structure of tropical soundscapes with intensifying land use in borneo. *Science of the Total Environment*, 852, 158268.
- Burivalova, Z., Orndorff, S., Truskinger, A., Roe, P., & Game, E. T. (2021). The sound of logging: Tropical forest soundscape before, during, and after selective timber extraction. *Biological Conservation*, 254, 108812.
- Bush, A., Sollmann, R., Wilting, A., Bohmann, K., Cole, B., Balzter, H., Martius, C., Zlinszky, A., Calvignac-Spencer, S., Cobbold, C. A., Dawson, T. P., Emerson, B. C., Ferrier, S., Gilbert, M. T. P., Herold, M., Jones, L., Leendertz, F. H., Matthews, L., Millington, J. D. A., ... Yu, D. W. (2017). Connecting earth observation to high-throughput biodiversity data. *Nature Ecology & Evolution*, 1(7), 0176.
- Bush, E. R., Abernethy, K. A., Jeffery, K., Tutin, C., White, L., Dimoto, E., Dikangadissi, J.-T., Jump, A. S., & Bunnefeld, N. (2017). Fourier analysis to detect phenological cycles using long-term tropical field data and simulations. *Methods in Ecology and Evolution*, 8(5), 530–540.
- Butsic, V., Lewis, D. J., Radeloff, V. C., Baumann, M., & Kummerle, T. (2017). Quasi-experimental methods enable stronger inferences from observational data in ecology. *Basic and Applied Ecology*, 19, 1–10.
- Buxton, R. T., McKenna, M. F., Clapp, M., Meyer, E., Stabenau, E., Angeloni, L. M., Crooks, K., & Wittemyer, G. (2018). Efficacy of extracting indices from large-scale acoustic recordings to monitor biodiversity. *Conservation Biology*, 32(5), 1174–1184.
- Carpenter, S. R., & Brock, W. A. (2006). Rising variance: A leading indicator of ecological transition. *Ecology Letters*, 9(3), 311–318.
- Chave, A. D. (2019). A multitaper spectral estimator for time series with missing data. *Geophysical Journal International*, 218, 2165–2178.
- Davis, C. C., Lyra, G. M., Park, D. S., Asprino, R., Maruyama, R., Torquato, D., Cook, B. I., & Ellison, A. M. (2022). New directions in tropical phenology. *Trends in Ecology & Evolution*, 37, 683–693.
- Dornelas, M., Gotelli, N. J., McGill, B., Shimadzu, H., Moyes, F., Sievers, C., & Magurran, A. E. (2014). Assemblage time series reveal biodiversity change but not systematic loss. *Science*, 344(6181), 296–299.
- Downey, H., Bretagnolle, V., Brick, C., Bulman, C. R., Cooke, S. J., Dean, M., Edmonds, B., Frick, W. F., Friedman, K., McNicol, C., Nichols, C., Herbert, S., O'Brien, D., Ockendon, N., Petrovan, S., Stroud, D., White, T. B., Worthington, T. A., & Sutherland, W. J. (2022). Principles for the production of evidence-based guidance for conservation actions. *Conservation Science and Practice*, 4(5), e12663.
- Dröge, S., Martin, D. A., Andriafanomezantsoa, R., Burivalova, Z., Fulgence, T. R., Osen, K., Rakotomalala, E., Schwab, D., Wurz, A., Richter, T., & Kreft, H. (2021). Listening to a changing landscape: Acoustic indices reflect bird species richness and plot-scale vegetation structure across different land-use types in north-eastern Madagascar. *Ecological Indicators*, 120, 106929.
- Fuller, S., Axel, A. C., Tucker, D., & Gage, S. H. (2015). Connecting soundscape to landscape: Which acoustic index best describes landscape configuration? *Ecological Indicators*, 58, 207–215.
- Gage, S. H., & Axel, A. C. (2014). Visualization of temporal change in soundscape power of a Michigan lake habitat over a 4-year period. *Ecological Informatics*, 21, 100–109.
- Gage, S. H., Wimmer, J., Tarrant, T., & Grace, P. R. (2017). Acoustic patterns at the samford ecological research facility in south east queensland, Australia: The peri-urban supersite of the terrestrial ecosystem research network. *Ecological Informatics*, 38, 62–75.
- Gaynor, K. M., Hohnowski, C. E., Carter, N. H., & Brashares, J. S. (2018). The influence of human disturbance on wildlife nocturnality. *Science*, 360(6394), 1232–1235.
- Gil, D., & Lusua, D. (2020). The bird dawn chorus revisited. In *Coding strategies in vertebrate acoustic communication* (Vol. 7, pp. 45–90). Springer Nature.
- Gilbert, N. A., McGinn, K. A., Nunes, L. A., Shipley, A. A., Bernath-Plaisted, J., Clare, J. D., Murphy, P. W., Keyser, S. R., Thompson, K. L., Nelson, S. B. M., Cohen, J. M., Widick, I. V., Bartel, S. L., Orrock, J. L., & Zuckerman, B. (2022). Daily activity timing in the anthropocene. *Trends in Ecology & Evolution*, 38(4), 324–336.
- Gleich, S. J., Cram, J. A., Weissman, J. L., & Caron, D. A. (2022). Netgam: Using generalized additive models to improve the predictive power of ecological network analyses constructed using time-series data. *ISME Communications*, 2(1), 23.
- Gottesman, B. L., Olson, J. C., Yang, S., Acevedo-Charry, O., Francomano, D., Martinez, F. A., Appeldoorn, R. S., Mason, D. M., Weil, E., & Pijanowski, B. C. (2021). What does resilience sound like? Coral reef and dry forest acoustic communities respond differently to Hurricane Maria. *Ecological Indicators*, 126, 107635.
- Guisan, A., Edwards, T. C., Jr., & Hastie, T. (2002). Generalized linear and generalized additive models in studies of species distributions: Setting the scene. *Ecological Modelling*, 157(2–3), 89–100.
- Häfker, N. S., & Tessmar-Raible, K. (2020). Rhythms of behavior: Are the times changin'? *Current Opinion in Neurobiology*, 60, 55–66.
- Haley, C. L. (2021). Missing-data multitaper coherence estimation. *IEEE Signal Processing Letters*, 28, 1704–1708.
- Hammer, Ø. (2007). Spectral analysis of a plio-pleistocene multispecies time series using the mantel periodogram. *Palaeogeography, Palaeoclimatology, Palaeoecology*, 243(3–4), 373–377.
- Hastie, T., & Tibshirani, R. (1990). *Generalized additive models* (Chapman & Hall/CRC monographs on statistics & applied probability). Chapman and Hall/CRC.
- Hegg, J. C., & Kennedy, B. P. (2021). Let's do the time warp again: Non-linear time series matching as a tool for sequentially structured data in ecology. *Ecosphere*, 12(9), e03742.
- Hillebrand, H., Blasius, B., Borer, E. T., Chase, J. M., Downing, J. A., Eriksson, B. K., Filstrup, C. T., Harpole, W. S., Hodapp, D., Larsen, S., Lewandowska, A. M., Seabloom, E. W., van de Waal, D. B., & Ryabov, A. B. (2018). Biodiversity change is uncoupled from species richness trends: Consequences for conservation and monitoring. *Journal of Applied Ecology*, 55(1), 169–184.
- Ince, L. M. (2022). Introduction to biological rhythms: A brief history of chronobiology and its relevance to parasite immunology. *Parasite Immunology*, 44(3), e12905.
- Inouye, D. W. (2022). Climate change and phenology. *Wiley Interdisciplinary Reviews: Climate Change*, 13(3), e764.
- Koopmans, L. H. (1995a). *The spectral analysis of time series* (2nd ed.). Academic Press.
- Koopmans, L. H. (1995b). *The spectral analysis of time series*. Elsevier.
- Lawson, J., Whitworth, A., & Banks-Leite, C. (2022). Soundscapes show disruption across the diel cycle in human modified tropical landscapes. *Ecological Indicators*, 144, 109413.
- Lewińska, K. E., Ives, A. R., Morrow, C. J., Rogova, N., Yin, H., Elsen, P. R., de Beurs, K., Hostert, P., & Radeloff, V. C. (2023). Beyond "greening" and "browning": Trends in grassland ground cover fractions across eurasia that account for spatial and temporal autocorrelation. *Global Change Biology*, 29(16), 4620–4637.
- Magurran, A. E., Baillie, S. R., Buckland, S. T., Dick, J. M., Elston, D. A., Scott, E. M., Smith, R. I., Somerfield, P. J., & Watt, A. D. (2010). Long-term datasets in biodiversity research and monitoring: Assessing change in ecological communities through time. *Trends in Ecology & Evolution*, 25(10), 574–582.
- Mann, M. E., & Park, J. (1999). Oscillatory spatiotemporal signal detection in climate studies: A multiple-taper spectral domain approach. *Advances in Geophysics*, 41, 1–131.
- Martin, P. A., Christie, A. P., Shackelford, G. E., Hood, A. S., Wang, S., Li, B., Morgan, W., Lee, M., Aldridge, D. C., & Sutherland, W. J. (2023). Flexible synthesis can deliver more tailored and timely evidence for research and policy. *Proceedings of the National Academy of Sciences of the United States of America*, 120(25), e222191120.
- Martinez-Bakker, M., & Helm, B. (2015). The influence of biological rhythms on host–parasite interactions. *Trends in Ecology & Evolution*, 30(6), 314–326.

- Metcalfe, O. C., Barlow, J., Devenish, C., Marsden, S., Berenguer, E., & Lees, A. C. (2021). Acoustic indices perform better when applied at ecologically meaningful time and frequency scales. *Methods in Ecology and Evolution*, 12(3), 421–431.
- Monahan, W. B., Rosemartin, A., Gerst, K. L., Fisichelli, N. A., Ault, T., Schwartz, M. D., Gross, J. E., & Weltzin, J. F. (2016). Climate change is advancing spring onset across the us national park system. *Ecosphere*, 7(10), e01465.
- Morisette, J. T., Richardson, A. D., Knapp, A. K., Fisher, J. I., Graham, E. A., Abatzoglou, J., Wilson, B. E., Breshears, D. D., Henebry, G. M., Hanes, J. M., & Liang, L. (2009). Tracking the rhythm of the seasons in the face of global change: Phenological research in the 21st century. *Frontiers in Ecology and the Environment*, 7(5), 253–260.
- Müller, J., Mitesser, O., Schaefer, H. M., Seibold, S., Busse, A., Kriegel, P., Rabl, D., Gelis, R., Arteaga, A., Freile, J., Leite, G. A., de Melo, T. N., LeBien, J., Campos-Cerqueira, M., Blüthgen, N., Tremlett, C. J., Böttger, D., Feldhaar, H., Grella, N., ... Buřivalová, Z. (2023). Soundscapes and deep learning enable tracking biodiversity recovery in tropical forests. *Nature Communications*, 14(1), 6191.
- Nun, I., Protopapas, P., Sim, B., Zhu, M., Dave, R., Castro, N., & Pichara, K. (2015). *Fats: Feature analysis for time series*. arXiv:1506.00010.
- Pedersen, E. J., Miller, D. L., Simpson, G. L., & Ross, N. (2019). Hierarchical generalized additive models in ecology: An introduction with mgcv. *PeerJ*, 7, e6876.
- Percival, D. B., & Walden, A. T. (2020). *Spectral analysis for physical applications: Multitaper and conventional univariate techniques*. Cambridge University Press.
- Planque, R., & Slabbekoorn, H. (2008). Spectral overlap in songs and temporal avoidance in a peruvian bird assemblage. *Ethology*, 114(3), 262–271.
- Pokrovsky, I., Kölzsch, A., Sherub, S., Fiedler, W., Glazov, P., Kulikova, O., Wikelski, M., & Flack, A. (2021). Longer days enable higher diurnal activity for migratory birds. *Journal of Animal Ecology*, 90(9), 2161–2171.
- R Core Team. (2023). *R: A language and environment for statistical computing*. R Foundation for Statistical Computing.
- Rahim, K., & Burr, W. (2013). *multitaper: Multitaper spectral analysis tools*. R package version 1.0-8.
- Rasmussen, C. E., & Williams, C. K. I. (2006). *Gaussian processes for machine learning, volume 1*. MIT press Cambridge.
- Ravindra, K., Rattan, P., Mor, S., & Aggarwal, A. N. (2019). Generalized additive models: Building evidence of air pollution, climate change and human health. *Environment International*, 132, 104987.
- Recuero, L., Litago, J., Pinzón, J. E., Huesca, M., Moyano, M. C., & Palacios-Orueta, A. (2019). Mapping periodic patterns of global vegetation based on spectral analysis of ndvi time series. *Remote Sensing*, 11(21), 2497.
- Roe, P., Eichinski, P., Fuller, R. A., McDonald, P. G., Schwarzkopf, L., Towsey, M., Trusking, A., Tucker, D., & Watson, D. M. (2021). The australian acoustic observatory. *Methods in Ecology and Evolution*, 12(10), 1802–1808.
- Sakai, S., & Kitajima, K. (2019). Tropical phenology: Recent advances and perspectives. *Ecological Research*, 34(1), 50–54.
- Salazar, J. E., Benavides, I. F., Cabrera, C. V. P., Guzmán, A. I., & Selvaraj, J. J. (2021). Generalized additive models with delayed effects and spatial autocorrelation patterns to improve the spatiotemporal prediction of the skipjack (*Katsuwonus pelamis*) distribution in the colombian Pacific ocean. *Regional Studies in Marine Science*, 45, 101829.
- Scarpelli, M. D., Lique, B., Tucker, D., Fuller, S., & Roe, P. (2021). Multi-index ecoacoustics analysis for terrestrial soundscapes: A new semi-automated approach using time-series motif discovery and random forest classification. *Frontiers in Ecology and Evolution*, 9, 738537.
- Schaller, C., Göckede, M., & Foken, T. (2017). Flux calculation of short turbulent events—comparison of three methods. *Atmospheric Measurement Techniques*, 10(3), 869–880.
- Sethi, S. S., Jones, N. S., Fulcher, B. D., Picinali, L., Clink, D. J., Klinck, H., Orme, C. D. L., Wrege, P. H., & Ewers, R. M. (2020). Characterizing soundscapes across diverse ecosystems using a universal acoustic feature set. *Proceedings of the National Academy of Sciences of the United States of America*, 117(29), 17049–17055.
- Shumway, R. H., Stoffer, D. S., & Stoffer, D. S. (2000). *Time series analysis and its applications, volume 3*. Springer.
- Slepian, D. (1978). Prolate spheroidal wave functions, Fourier analysis, and uncertainty V: The discrete case. *Bell System Technical Journal*, 57(5), 1371–1429.
- Socolar, J. B., Gilroy, J. J., Kunin, W. E., & Edwards, D. P. (2016). How should beta-diversity inform biodiversity conservation? *Trends in Ecology & Evolution*, 31(1), 67–80.
- Soleymani, A., Pennekamp, F., Dodge, S., & Weibel, R. (2017). Characterizing change points and continuous transitions in movement behaviours using wavelet decomposition. *Methods in Ecology and Evolution*, 8(9), 1113–1123.
- Stein, M. L. (2005). Statistical methods for regular monitoring data. *Journal of the Royal Statistical Society, Series B: Statistical Methodology*, 67(5), 667–687.
- Stoffer, D., & Poison, N. (2024). *astsa: Applied statistical time series analysis*. R package version 2.1.
- Stoy, P. C., Dietze, M. C., Richardson, A. D., Vargas, R., Barr, A. G., Anderson, R., Arain, M. A., Baker, I. T., Black, T. A., Chen, J. M., Cook, R. B., Gough, C. M., Grant, R. F., Hollinger, D. Y., Izaurralde, R. C., Kucharik, C. J., Lafleur, P., Law, B. E., Liu, S., ... Weng, E. (2013). Evaluating the agreement between measurements and models of net ecosystem exchange at different times and timescales using wavelet coherence: An example using data from the north american carbon program site-level interim synthesis. *Biogeosciences*, 10(11), 6893–6909.
- Thomson, D. J. (1982). Spectrum estimation and harmonic analysis. *Proceedings of the IEEE*, 70(9), 1055–1096.
- Towsey, M., Trusking, A., Cottman-Fields, M., & Roe, P. (2020). Qutecoacoustics/audio-analysis: Ecoacoustics audio analysis software (v20.11.2.0). Zenodo.
- Towsey, M., Zhang, L., Cottman-Fields, M., Wimmer, J., Zhang, J., & Roe, P. (2014). Visualization of long-duration acoustic recordings of the environment. *Procedia Computer Science*, 29, 703–712.
- Vega-Hidalgo, A., Flatt, E., Whitworth, A., & Symes, L. (2021). Acoustic assessment of experimental reforestation in a costa rican rainforest. *Ecological Indicators*, 133, 108413.
- Wauchope, H. S., Amano, T., Geldmann, J., Johnston, A., Simmons, B. I., Sutherland, W. J., & Jones, J. P. (2021). Evaluating impact using time-series data. *Trends in Ecology & Evolution*, 36(3), 196–205.
- White, E. R., & Hastings, A. (2020). Seasonality in ecology: Progress and prospects in theory. *Ecological Complexity*, 44, 100867.
- Williams, H. J., Taylor, L. A., Benhamou, S., Bijleveld, A. I., Clay, T. A., de Grissac, S., Demšar, U., English, H. M., Franconi, N., Gómez-Laich, A., Griffiths, R. C., Kay, W. P., Morales, J. M., Potts, J. R., Rogerson, K. F., Rutz, C., Spelt, A., Trevail, A. M., Wilson, R. P., & Börger, L. (2020). Optimizing the use of biologgers for movement ecology research. *Journal of Animal Ecology*, 89(1), 186–206.
- Wuethrich, B. (2000). How climate change alters rhythms of the wild. *Science*, 287(5454), 793–795.
- Yoh, N., Haley, C. L., & Buřivalová, Z. (2024a). Data for time series analysis for cyclical ecological data [dataset]. <https://doi.org/10.5061/dryad.xpvnvXOkn6>
- Yoh, N., Haley, C. L., & Buřivalová, Z. (2024b). Tallyyoh/timeseriesecocycles: Times series methods for the analysis of soundscapes and other cyclical ecological data (v1.0.1). <https://doi.org/10.5281/zenodo.11198178>

Yoh, N., Mbamy, W., Gottesman, B. L., Froese, G. Z. L., Satchivi, T., Obiang Ebanega, M., Carson, L., Ekazama Koto, S., Ozdogan, M., Seaman, D. J. I., Maicher, V., Malinowski, H., Poulsen, J., Ebang Mbélé, A., & Buřivalová, Z. (2024). *Impacts of logging, hunting, and conservation on vocalizing biodiversity in Gabon*. SSRN.

SUPPORTING INFORMATION

Additional supporting information can be found online in the Supporting Information section at the end of this article.

Table S1. The R-squared, mean, and variance for the acoustic index Power Minus Noise for the eight rainforest sites from Gabon.

Figure S1. Waveforms generated for Power Minus Noise (PMN)

across the day atop of hourly boxplots generated for PMN for each of the sites.

How to cite this article: Yoh, N., Haley, C. L., & Burivalova, Z. (2024). Time series methods for the analysis of soundscapes and other cyclical ecological data. *Methods in Ecology and Evolution*, 00, 1–19. <https://doi.org/10.1111/2041-210X.14361>